

Evolution of Mitochondrion-related Organelles in Metamonada

January 2019

Keitaro KUME

Evolution of Mitochondrion-related Organelles in Metamonada

A Dissertation Submitted to
the Graduate School of Life and Environmental Sciences,
the University of Tsukuba
in Partial Fulfillment of the Requirements
for the Degree of Doctor of Philosophy in Science
(Doctoral Program in Biological Sciences)

Keitaro KUME

1 Abstract

2 Evolution of mitochondria is one of most intensively studied areas of biology.
3 Mitochondria are organelles found in nearly all of eukaryotes, and arose through an
4 endosymbiotic event in which ancestral eukaryotes engulfed a bacterium closely related
5 to extant α -proteobacteria. For the last two decades, unusual and divergent
6 mitochondria have been reported from various lineages. Their organelles were shown to
7 be of mitochondrial origin, but they lacked aerobic respiration functions and/or their
8 own genomes. These reductive organelles are currently known as mitochondrion-related
9 organelles (MROs). Metamonada, a major clade of eukaryotes, is an important lineage
10 for studying the reductive evolution of mitochondria, because nearly all metamonads
11 appear to contain MROs rather than typical mitochondria and their phylogenetic
12 relationships have been clearly resolved. Additionally, the MROs of metamonad
13 parasites, including *Trichomonas vaginalis*, *Giardia intestinalis*, and *Spiroplasma*
14 *salmonicida* have been well studied in the proteomics level.

15 Although various functions are known in typical mitochondria, previous
16 studies of the evolution of MROs in metamonads have mainly focused on functions
17 related to energy metabolism. In the first comparative transcriptome study,
18 contamination of bacterial sequences in the metamonad transcriptome data sometimes
19 interfered with correctly annotating mitochondria/MRO-related proteins, as
20 mitochondria have a bacterial origin. In addition, absence of reliable methods for
21 predicting whether a given protein is a mitochondrial/MRO protein or not was critical
22 issue when discussing what the functions are the mitochondrion/MRO really has.

42 List of abbreviations

Abbreviations (Abb.)	Descriptions	Abb.	Descriptions
ATP	Adenosine triphosphate	GDH	Glutamate dehydrogenase
AUC	Area under the curve	GrpE	molecular chaperone GrpE
CLO	Carpediemonas-like organism	Grx5	Glutaredoxin-5
DNA	Deoxyribonucleic acid	HCP	Hybrid cluster protein
EST	Expressed sequence tag	HscB	molecular chaperone HscB
GBM	Gradient boosting machine	Hsp70	heat shock protein 70
HMM	hidden Markov model	HydE	Fe-hydrogenase Maturase E
ISC	Iron sulfur cluster	HydF	Fe-hydrogenase Maturase F
LGT	Lateral gene transfer	HydG	Fe-hydrogenase Maturase G
MRO	Mitochondrion-related organelle	IscA	Iron-sulfur cluster assembly
Mt	Mitochondria	IscS	Cysteine desulfurase IscS
NGS	Next generation sequencing	IscU	Iron-sulfur cluster assembly enzyme ISCU
RNA	Ribonucleic acid	MDH	Malate dehydrogenase
ROC	Receiver operating characteristics	ME	Malic enzyme
SVM	Support vector machine	MGL	Methionine gamma lyase
		MPP	Mitochondrial processing peptidase
AAT	Asparate aminotransferase	NFU	Iron-sulfur cluster scaffold protein NFU
ACS	Acetyl CoA Synthase	NuoE	NADH:ubiquinone dehydrogenase E
AD	Arginine deminase	NuoF	NADH:ubiquinone dehydrogenase F
AK	Adenylate kinase	OCDA	Ornithine cyclodeaminase
ALT	Alanine aminotransferase	OCT	Ornithine carbamoyltransferase
ASCT	Acetate:succinate CoA transferase	PFO	Pyruvate:ferredoxin oxidoreductase
Cpn60	Heat shock protein 60	PSAT	Phosphoserine aminotransferase
CS	Cysteine syntase	Rbr	Rubrerythrin
Fdx	Ferredoxin	Rxn	Rubredoxin
FDXR	Adrenodoxin-NADP+ reductase	SCS	Succinyl coenzyme A (CoA) synthetase
Fe Hase	Fe only hydrogenase	SHMT	Serine hydroxymethyltransferase
Fxn	Frataxin	SOD	Superoxide dismutase
GCS H	Glycine cleavage system H-protein	Tnase	Tryptophanase
GCS L	Glycine cleavage system L-Protein	Trx	Thioredoxin
GCS P	Glycine cleavage system P-protein	TrxP	Thioredoxin Peroxidase
GCS T	Glycine cleavage system T-protein	TrxR	Thioledoxin reductase

43

44 Chapter 1. General introduction

45 1.1. Origin of mitochondria and its roles

46 Nearly all eukaryotes possess mitochondria, which are the double-membraned
47 organelles. Although the endosymbiotic origin of mitochondria remains controversial
48 (Andersson et al., 1998; Embley & Martin, 2006, Williams et al., 2007; Brindefalk et
49 al., 2011; Gray, 2012; Pittis & Gabaldón, 2016; Martin et al., 2017; Martijn et al., 2018),
50 it is widely accepted that a bacterium closely related to extant α -proteobacteria was
51 engulfed by an ancestral eukaryotic host, giving rise to mitochondria. These organelles
52 are responsible for various essential processes in the eukaryotic cells, such as aerobic
53 energy metabolism, iron sulfur clusters (ISC) (Fe-S clusters) assembly, fatty acid
54 metabolism, molecular chaperone system, anti-oxidant system, amino acid metabolism
55 and apoptosis.

56 Mitochondria of extant species contain their own genome (mtDNA) typically
57 composed of less than 100 genes coding for proteins and RNAs that function in
58 mitochondria. Because most of the genes encoding mitochondrial proteins related to
59 these biological processes are mainly located in the nuclear genome, these proteins must
60 be translocated into the mitochondria by protein sorting and transport systems that
61 recognize the mitochondrial targeting signal typically found in their N-terminal regions.
62 This selective transport causes the concentration of mitochondrial proteins be in high
63 concentration inside the mitochondria and maintains the efficiency of various enzymatic
64 reactions.

65 The acquisition of mitochondria enabled aerobic respiration with high
66 throughput energy production in ancestral eukaryotes, leading to the prosperity of

67 eukaryotes. However, the ability of aerobic respiration is one of the benefits by
68 mitochondria. In addition to aerobic energy metabolism mitochondria have been playing
69 other essential roles in the process of eukaryotic cellular evolution through the above
70 mentioned functions derived originally from α -proteobacteria.

71 1.2. Previous research for mitochondrial/mitochondrion-related 72 organelle proteins in Metamonada

73 During the evolutionary process of eukaryotes, mitochondria have diverged extensively.
74 Hydrogenosomes in *Trichomonas vaginalis* and mitosomes in *Giardia intestinalis* are
75 typical examples of highly divergent mitochondria (Morrison et al., 2007; Jedelský et
76 al., 2011; Schneider et al., 2011). These organelles are of mitochondrial origin, but they
77 lack their own genomes and most of nuclear genome-encoded mitochondrial proteins
78 related to the respiratory chain. These reductive organelles are currently referred to as
79 mitochondrion-related organelles (MROs). Recently it was proposed that
80 mitochondria/MROs should be classified into five functional types (Müller et al., 2012):
81 aerobic mitochondria (Class 1), anaerobic mitochondria (Class 2), H₂-producing
82 mitochondria (Class 3), hydrogenosomes (Class 4), and mitosomes (Class 5). In general,
83 MROs are involved in Class 4 or Class 5. Various types of MROs have been identified
84 in phylogenetically independent lineages which grow in micro-aerobic and anaerobic
85 environments, indicating that these organelles arose independently several times
86 throughout eukaryotic evolution (Roger et al., 2017). Metamonada is a large assemblage
87 of flagellates adapted to microaerophilic/anaerobic environments. The monophyly and
88 branching order of metamonads was robustly resolved by a recent phylogenomic
89 analysis (Leger et al., 2017) (Figure 1-1). Notably, nearly all metamonads appear to

90 possess MROs rather than typical aerobic mitochondria, indicating that analyses of
91 metamonads can provide valuable information regarding the evolutionary process of
92 MROs. Particularly, MROs of the ancestral metamonad lineage may have exhibited
93 functions typical of those in the mitochondria, while those of derived lineages may have
94 diverged towards reducing functions such as those in the mitosome of *Giardia* (Leger et
95 al., 2017).

96 1.2.1. Metamonada

97 Metamonada is a major clade in Excavata, a large taxonomic group of eukaryotes (Adl
98 et al., 2018). Metamonada consist of microaerophilic or anaerobic flagellates with
99 various lifestyles, such as heterotrophic free-living, commensal, or parasitic. There are
100 three sub clades of Metamonada, Preaxostyla, Parabasalia and Fornicata, exist with
101 Preaxostyla as an early branching clade.

102 1.2.2. Preaxostyla

103 Transcriptome analyses were performed on two protists in Preaxostyla, *Trimastix*
104 *marina* and *Paratrimastix pyriformi*. The data revealed the presence of mitochondrial
105 protein homologs related to the functions of amino acid metabolism and pyruvate
106 metabolism, suggesting that their putative MROs have these functions. However, the
107 presence or absence of other mitochondrion derived functions in the MROs could not be
108 concluded and their functions still remain unclear (Leger et al., 2017; Zubáčová et al.,
109 2013). Notably, *Monocercomonoides* sp. was the first eukaryote which was reported to
110 have neither mitochondria nor MRO. Genome and transcriptome data of
111 *Monocercomonoides* sp. are available in a public database (Karnkowska et al., 2016).
112 Although MRO was not identified morphologically, the presence of mitochondrion-
113 related chaperon proteins such as CPN60 (chaperonin 60) suggested the secondary

114 absence of MROs in the line leading to *Monocercomonoides* sp. (Karnkowska et al.,
115 2016).

116 1.2.3. Parabasalia

117 Genome and/or transcriptome sequence data were reported from hydrogenosome-
118 containing parasites/commensals, *Tritrichomonas foetus*, *Trichomonas vaginalis* and
119 *Pentatrichomonas hominis* in Parabasalia. More than four decades ago hydrogenosomes
120 were discovered in *T. foetus* and *T. vaginalis*, but these were not recognized as MROs at
121 that time (Lindmark & Müller 1973). Because *T. vaginalis* and *T. foetus* are important
122 parasites in the medical or veterinary field, their biological characteristics and MRO
123 features have been studied to a certain extent (Beltrán et al., 2013; Birkeland et al.,
124 2010; Carlton et al., 2007; Franzén et al., 2009; Jedelský et al., 2011; Schneider et al.,
125 2011). Based on biochemical, proteomic, genome and transcriptome analyses performed
126 for both *T. foetus* and *T. vaginalis*, the trichomonad hydrogenosomes were shown to
127 have lost their own genomes, parts of mitochondrial proteins and the ability to generate
128 ATP by oxidative phosphorylation, whereas they possess Fe-S cluster assembly, amino
129 acid metabolism and antioxidant systems (Schneider et al., 2011).

130 1.2.4. Fornicata

131 Fornicata consists of three taxonomic subgroups, diplomonads, retortamonads and
132 *Carpediemonas*-like organisms (CLOs), but only diplomonads are monophyletic (Adl et
133 al., 2018; Kolisko et al., 2010; Simpson 2003). Diplomonads include mammalian and
134 fish parasites, such as *Giardia intestinalis*, *Spironucleus salmonicida*, *S. barkhanus*, *S.*
135 *vortens*, and free-living flagellates classified to the genus *Trepomonas* or *Hexamita*.
136 Morphological studies by electron microscopy showed that all of the fornicate
137 organisms analyzed up to date do not contain typical mitochondria but do MROs:

138 previous studies have examined CLOs (Kolisko et al., 2010; Park et al., 2009; Yubuki et
139 al., 2013; Yubuki et al., 2007), *G. intestinalis* (Tovar et al., 2003), *S. salmonicida*
140 (Jerlström-Hultqvist et al., 2013), and *S. vortens* (Millet et al., 2013).

141 Genome and transcriptome analyses and proteomic analyses of MRO have
142 been conducted for the human parasite *G. intestinalis* and a fish parasite *S. salmonicida*,
143 indicating that these parasites possess highly derived MROs with reduced functions.
144 Particularly, in the evolution leading to *Giardia*, the MRO (mitosome) lost most of its
145 mitochondrial functions, and has only retained the function of the Fe-S cluster assembly
146 (Jedelský et al., 2011; Morrison et al., 2007; Tovar et al., 2003).

147 Transcriptome data were reported for *Chilomastix cuspidata* and *Chilomatix*
148 *caulleryi*, which are classified as retortamonads. Analyses of these data revealed that *C.*
149 *cuspidata* MRO may function in amino acid metabolism and NADH reoxidation, while
150 the MRO of *C. caulleryi*, a lumen-dwelling parasite, may have lost most of these
151 functions during its evolution (Leger et al., 2017).

152 CLOs are a polyphyletic group and include *Carpediemonas membranifera*,
153 *Ergobibamus cyprinoides*, *Aduncisulcus plauster*, *Kipferlia bialata* and *Dysnectes*
154 *brevis*. Transcriptome analyses have been conducted for these organisms (Leger et al.,
155 2017), and genomic analyses were performed for *K. bialata* (Tanifuji et al., 2018). Their
156 MROs were shown to retain functions of at least amino acid metabolism, ATP synthesis,
157 NADH reoxidation and H₂ production.

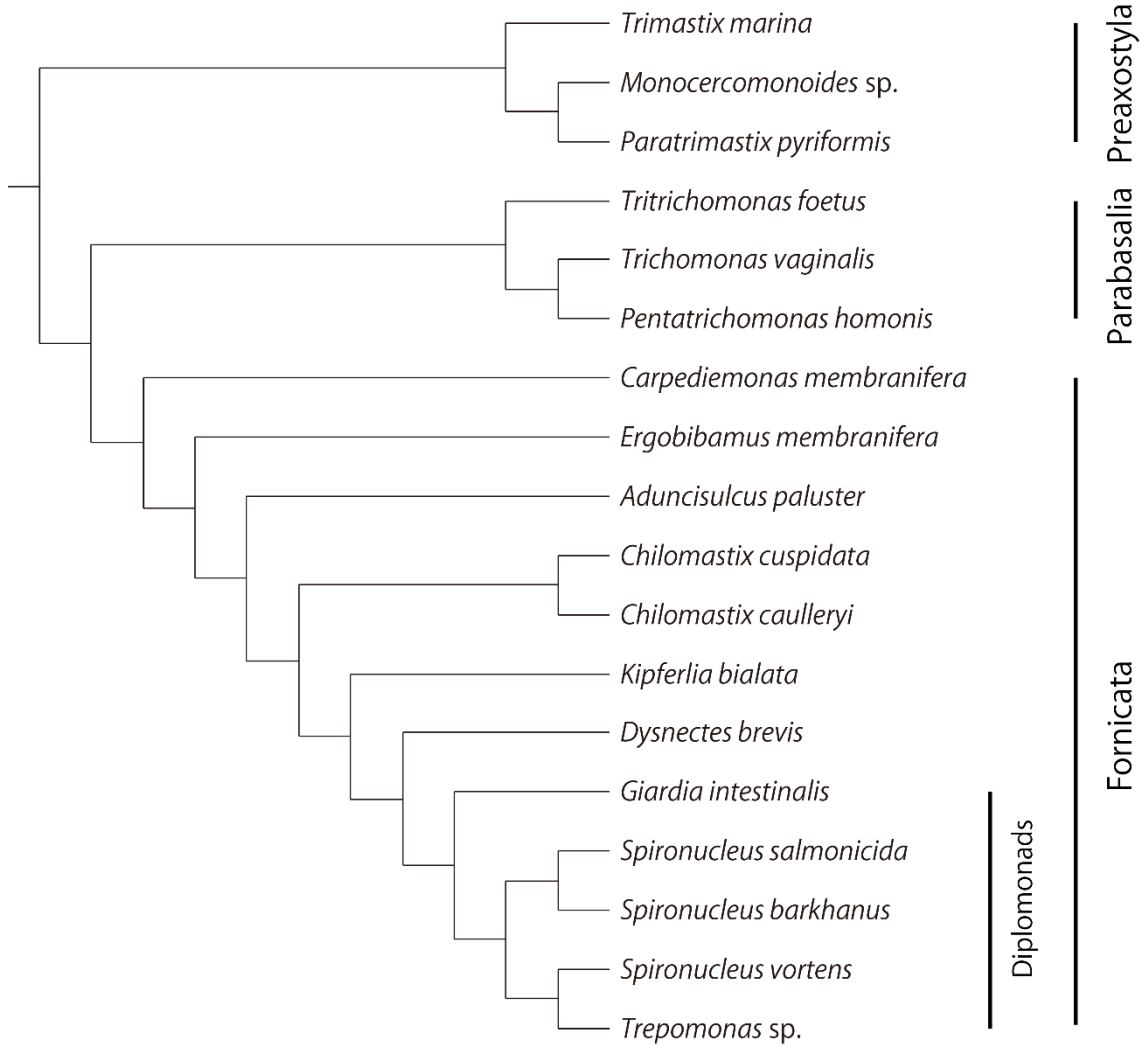
158 1.3. Application of bioinformatics method to the analysis of MRO 159 proteome

160 While transcriptome analyses have been performed for many metamonads, proteome
161 analyses of MRO have been conducted only for *T. foetus*, *T. vaginalis*, *G. intestinalis*
162 and *S. salmonicida* (Table 1-1). Because parasites are important in the medical,
163 veterinary and fishery fields, experimental procedures such as axenic culture, organelle
164 purification, and biochemical analysis have been established. However, these methods
165 have not been established yet for heterotrophic metamonads which must be cultured
166 with bacterial feed. Developing these methods for a direct proteome analysis of MROs
167 is very difficult because of the contamination with bacteria in the materials used for
168 molecular analyses. Thus, it is necessary to distinguish mitochondrial/MRO proteins
169 from other proteins using various bioinformatics methods.

170 Transcriptome data for heterotrophic metamonads such as *K. bialata* and *D.*
171 *brevis* were generated from non-axenic cultures in a previous study by Leger et al.
172 (2017). Bacterial contamination resulted in a low quality of assembly and a small
173 amount of eukaryotic sequence data, preventing the detection of the presence or absence
174 of each mitochondrial/MRO protein in the putative MRO proteome. To improve the
175 quality of data, density gradient centrifugation was conducted to reduce bacterial
176 contamination for the genome and transcriptome analyses of *K bialata*, resulting in the
177 first report of a draft genome of heterotrophic metamonads (Tanifuji et al., 2018).

178 Most previous studies (Jedelský et al., 2011; Rada et al., 2011; Schneider et al.,
179 2011) used prediction software for mitochondrial proteins such as TargetP
180 (Emanuelsson et al., 2007), Tppred2 (Savojardo et al., 2014) and Mitofates (Fukasawa

217



218

Figure 1-1: Phylogenetic tree of Metamonada (Leger et al., 2017 modified into cladogram tree; 159 proteins, 39,089 sites, 94 taxa, CAT-GTR + Γ model.)

219

Table 1-1: List of previous omics studies for metamonads. A check mark (✓) indicates that the corresponding omics analysis was performed, and its data are available. A grey cell indicates that the data are unavailable or do not exist.

220

		Transcriptome	Genome	Proteome
Preaxostyla	<i>Trimastix marina</i>	✓		
	<i>Paratrimastix pyriformis</i>	✓		
	<i>Monocercomonoides</i> sp.	✓	✓	
Parabasalia	<i>Trichomonas vaginalis</i>	✓	✓	✓
	<i>Pentatrichomonas hominis</i>	✓	✓	✓
	<i>Tritrichomonas foetus</i>	✓	✓	✓
Fornicata	<i>Carpediemonas membranifera</i>	✓		
	<i>Iotanema spirale</i>	✓		
	<i>Ergobibamus cyprinoides</i>	✓		
	<i>Aduncisulcus paluster</i>	✓		
	<i>Chilomastix cuspidata</i>	✓		
	<i>Chilomastix caulleryi</i>	✓		
	<i>Kipferlia bialata</i>	✓	✓	
	<i>Dysnectes brevis</i>	✓		
	<i>Giardia intestinalis</i>	✓	✓	✓
	<i>Spironucleus salmonicida</i>	✓	✓	✓
	<i>Spironucleus barkhanus</i>	✓ (EST)		
	<i>Spirinucleus vortens</i>	✓ (EST)		
	<i>Trepomonas</i> sp.	✓		

221

401 Chapter 3. NommPred: Prediction of Mitochondrial and 402 Mitochondrion-related Organelle Proteins of 403 Non-model Organisms

404 3.1. Introduction

405 Mitochondria are separated from other cellular components by a double membrane,
406 resulting in the concentration of mitochondrial proteins inside the membrane. In
407 general, the functions of an organelle are determined by the protein repertoire of the
408 organelle. Therefore, the estimation of the function of mitochondria needs to determine
409 the repertoire of mitochondrial proteins, most of which are nuclear encoded, expressed
410 in cytosol, and finally transported into mitochondria (Gonczarowska-Jorge et al., 2017).

411 To determine a repertoire of mitochondrial proteins, the proteomic analysis of
412 mitochondria is essential. For model organisms, experimental methods for the
413 proteomic analysis of mitochondria have already been established during their long
414 research histories (Kumar et al., 2002; Sickmann et al., 2003; Reinders et al., 2006;
415 Cherry et al., 2012; Chen et al., 2010); however, for non-model organisms, there are no
416 general strategies for the proteomic analysis of mitochondria. Even in non-model
417 organisms, information on the amino acid sequences of proteins is indirectly obtained
418 from the nucleotide sequences of the genome or transcriptome analysis, and these are
419 useful tools for studying the cellular and molecular biological research subjects of non-
420 model organisms of which proteins are difficult to treat directly during experiments.
421 Recently, high throughput sequencing, the so-called next-generation sequencing (NGS),
422 has allowed us to easily obtain the entire genome or transcriptome data even from non-
423 model organisms at a low cost and in a short time. Therefore, transcriptome analysis is

424 performed for the entire cell extracts of non-model organisms including mitochondria
425 and the other cellular components, and the mitochondrial proteins are predicted by using
426 an amino acid sequence-based computational method instead of purifying mitochondria
427 and determining the repertoire of mitochondrial proteins directly. Such a bioinformatics
428 approach needs to discriminate mitochondrial proteins from all the proteins that are
429 deduced from the entire cell transcriptome data.

430 A machine learning approach has been often used to classify
431 mitochondrial/non-mitochondrial proteins. Various software programs based on
432 machine learning are available; these programs predict whether an input protein
433 sequence is a mitochondrial protein. For example, TPpred3 (Savojardo et al., 2015) and
434 Mitofates (Fukasawa et al., 2015) are prediction software programs based on support
435 vector machines, whereas TargetP (Emanuelsson et al., 2007) is a software program
436 based on neural network techniques.

437 Most of the current prediction software programs, including TPpred3,
438 Mitofates, and TargetP, are trained only with the data derived from model organisms,
439 which belong to the taxonomic groups, Metazoa, Fungi, or Embryophyta, and these
440 programs are designed for application to the proteins of model organisms and their
441 relatives. Model organisms have been studied experimentally at an enormous cost
442 because of their basic biological, medical, or industrial importance. This has resulted in
443 the accumulation of vast biochemical experimental data of protein localization to
444 cellular compartments including mitochondria.

445 On the other hand, in the case of non-model organisms, except for those that
446 are closely related to the known model organisms, very few experimental data are
447 available because of the shortage of basic experimental procedures although they

448 exhibit most parts of the eukaryotic diversities (Adl et al., 2018). Hereafter, I refer to
449 such non-model organisms that do not belong to Metazoa, Embryophyta, and Fungi as
450 non-model organisms. Therefore, for the study of the mitochondrial proteins derived
451 from non-model organisms, the sequence data of genome or transcriptome that are
452 produced by using the NGS approach are mainly used to predict the proteins that would
453 be mitochondrially localized. In general, the prediction tools designed for model
454 organisms are usually applied for these analyses; however, these tools do not necessarily
455 guarantee accuracy of prediction because the N-terminal sequence features important
456 for the prediction of the mitochondrial proteins could be far divergent in non-model
457 organisms compared to those of the model organisms. In particular, in the case of the
458 prediction of MRO protein, the prediction tools currently available are highly inaccurate
459 (Makiuchi & Nozaki, 2014). Therefore, in general, for predicting of
460 mitochondrial/MRO proteins in non-model organisms, the consensus of the results from
461 multiple predictors is considered to avoid false predictions. However, this cannot be
462 validated.

463 To resolve this problem, here, I propose a software program, NommPred (non-
464 model organismal mitochondrial/MRO protein predictor), which predicts the
465 mitochondrial/MRO proteins derived from non-model organisms. To develop this
466 software, I prepared a dataset including the mitochondrial or MRO proteins derived
467 widely from non-model organisms and adopted a gradient boosting machine (GBM)
468 (Friedman, 1999; Friedman et al., 2000; Friedman, 2002) as a classifier. GBM, which is
469 one of the ensemble classifiers, was used instead of the support vector machine (Cortes
470 & Vapnik, 1995), which was adopted in the previous predictors Mitofates and TPpred3.
471 NommPred could resolve the problem due to the inconsistency between the origins of

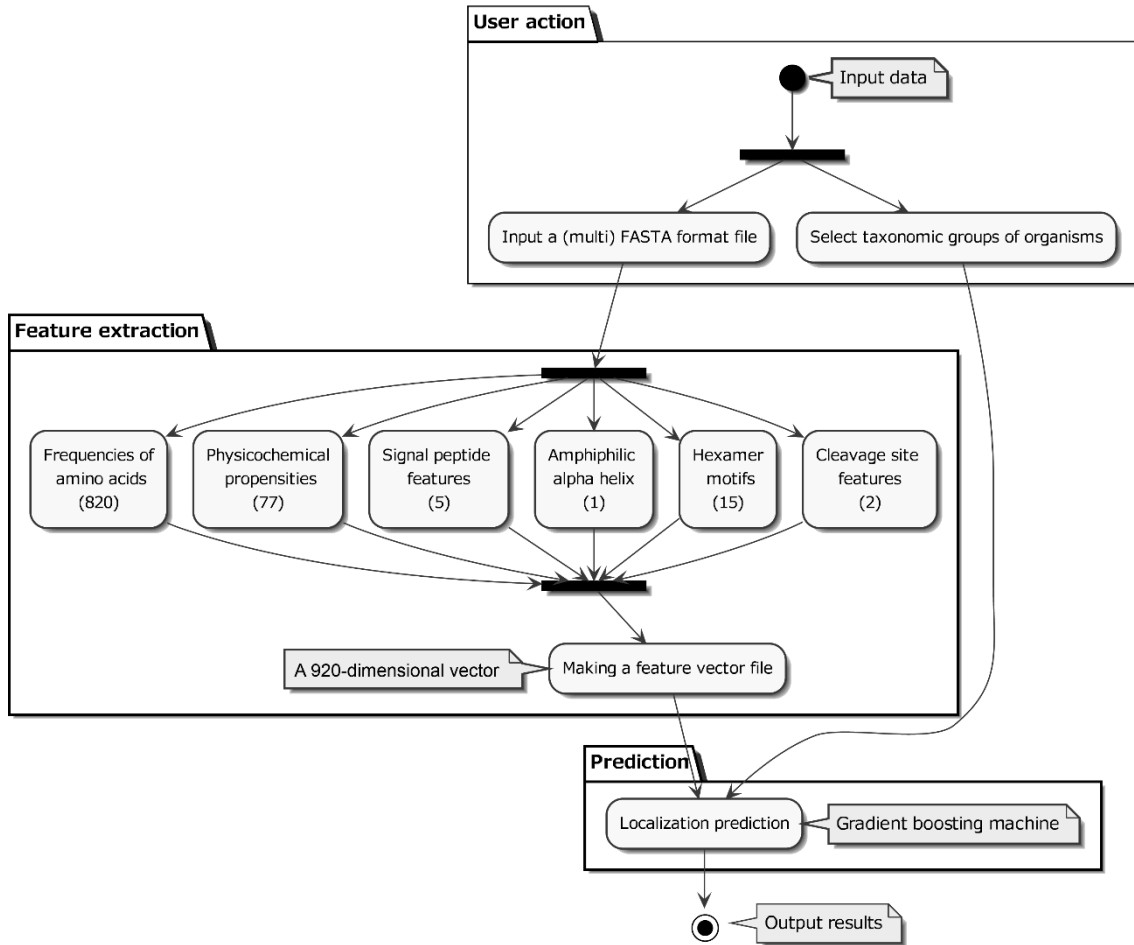
472 the training and input data when predicting the mitochondrial/MRO proteins of non-
473 model organisms. The performance of NommPred was shown to be superior to
474 Mitofates, which was demonstrated to be the best among the alternative methods, in
475 predicting the mitochondrial/MRO proteins derived from non-model organisms.
476 Therefore, NommPred is the best predictor for the mitochondrial/MRO proteins of non-
477 model organisms.

478 3.2. Materials and Methods

479 3.2.1. Scheme of NommPred

480 A flowchart and a message sequence chart of the newly developed software,
481 NommPred, are illustrated in Figures 3-1 and 3-2, respectively. The software takes as
482 input both the protein sequence in FASTA format (Definition is available from:
483 www.ncbi.nlm.nih.gov/books/NBK53702/) and organismal information from which the
484 protein sequence is derived. The feature of each protein was extracted based on
485 Mitofates' algorithm to create a 920-dimensional feature vector (Figure 3-1). The vector
486 is subjected to the GBM predictor (Mit Predictor for mitochondrial proteins or MRO
487 Predictor for MRO proteins as described below), and the predictor outputs the
488 prediction results and probabilities.

NommPred: Flow Chart

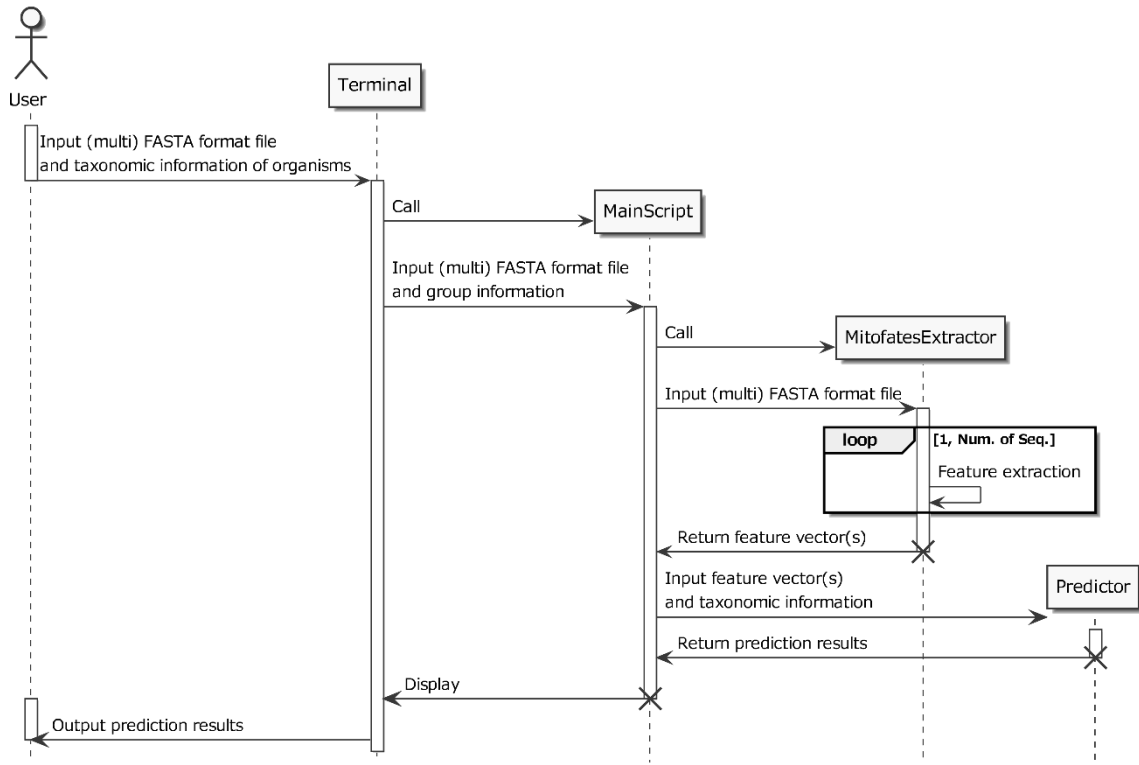


489

Figure 3-1: Flowchart of NommPred. The closed circle represents the starting point of the program, and the closed circle surrounded by a larger open circle represents the endpoint. The user input data (Input data) include the protein sequence in FASTA format and information of the protein sequence origin (taxonomic group). The input data are classified into (the first black bar in User action step) protein sequence, which is used for feature extraction, and organismal information, which is used for the selection of an appropriate GBM Predictor: Mit Predictor, MRO Predictor, or others. In the feature extraction step, the 920 calculated features (Table 3-1) are integrated, and a 920-dimensional feature vector is obtained as the output. In the figure, only six feature categories are depicted with the number of individual features. This vector is subjected to a selected GBM Predictor as the input data, and then the prediction result is shown (Output Results).

490

NommPred Prediction Sequence



491

Figure 3-2: Message sequence chart of NommPred. The software for NommPred is console user interface (CUI), and it runs on the terminal. The software accepts a protein sequence file in multi FASTA format and a text file with information of the origins of the sequences and outputs the prediction results at last.

492

493 3.2.2. Dataset construction

494 The dataset used for the training and test is shown in Table 3-1. The mitochondrial or
495 MRO proteins are treated as positive samples and the others as negative samples. The
496 sequence data were obtained from UniProt (UniProt C, 2017; www.uniprot.org/),
497 GiardiaDB (Hagen et al, 2011; Aurrecochea et al, 2009; giardiadb.org/giardiadb/),
498 TrichDB (Aurrecochea et al, 2009; trichdb.org/trichdb/), and ApiLoc (Woodcroft et al,
499 2011; apiloc.biochem.unimelb.edu.au/apiloc/apiloc). Although these databases
500 sometimes annotate mitochondrial or MRO proteins based on computational prediction,
501 I used only those proteins whose localization was confirmed experimentally (e.g.,
502 Westernblotting, immunoblotting, or fluorescence microscope analysis) to mitochondria
503 or MROs by investigating the literature. Then, I applied protein sequence redundancy
504 reduction by using the BLASTClust program from the NCBI BLAST packages
505 (Altschul et al, 1990). I adopted the criteria of being redundant at > 95% sequence
506 identity. Finally, I prepared 392 positive mitochondrial or MRO protein sequences and
507 3,739 negative sequences. I classified the entire dataset into mitochondrial and MRO
508 datasets, Mit and MRO. Then, I created a predictor for each dataset; one is the predictor
509 for the mitochondrial protein trained with the mitochondrial proteins of 7 non-model
510 organismal taxonomic groups (Mit Predictor), whereas the other is the predictor for the
511 MRO protein trained with the MRO proteins of three non-model organismal taxonomic
512 groups that possess MRO (groups marked with asterisks in Table 3-1) (MRO Predictor),
513 because these two datasets were expected to be apparently different in the N-terminal
514 sequence features of the mitochondrial/MRO protein sequences. The N-terminal
515 sequence features of the MRO proteins are generally considered to be extremely
516 divergent from those of the mitochondrial proteins.

Table 3-1: Entire dataset used for training and test. If the taxonomic group corresponds exactly to the genus, the name of the genus is represented in italic form. “Stramenopiles” is not a formal taxonomic rank but is generally used for the name of the group. The “Positive samples” column lists the number of sequences of the mitochondrial or MRO proteins. The “Negative samples” column lists the number of sequences of the non-mitochondrial or non-MRO proteins. The groups that possess MRO are represented with asterisks.

517

Taxonomic group	Positive samples	Negative samples
Chlorophyta	60	81
<i>Dictyostelium</i>	52	622
Piroplasma	7	387
<i>Plasmodium</i>	42	435
Stramenopiles	44	1029
<i>Toxoplasma</i>	30	125
Trypanosomatida	48	587
* <i>Entamoeba</i>	7	94
* <i>Giardia</i>	20	271
* <i>Trichomonas</i>	82	108
Total	392	3,739

518

519 3.2.3. Feature extraction

520 For the extraction of features, I used the method described in Fukazawa et al. (2015).

521 The feature of each protein was extracted to create a 920-dimensional feature vector.

522 Extracted features and its details are shown in Table 3-2.

523

Table 3-2: List of features. For more details, refer to Mitofates (Fukasawa et al., 2015).

Feature category	Number of features	Features	Description
Frequencies of amino acids	820	Monopeptide: X_1 Dipeptide: X_1X_2 Skip-two dipeptides: X_1xxX_2	Normalized frequencies for each of the possible combinations of the standard 20 amino acids in 30 N-terminal residues of the input sequences. X_i ($i = 1,2$) and small x represents standard 20 amino acids, A C D E F G H I K L M N P Q R S T V W Y.
Physicochemical propensities	77	Segment scores Whole score	90 N-terminal residues of the input sequence are divided into six segments. Segment scores are calculated for each of the six segments. The total score is the sum of the segment scores. Each score is computed for: the mean of 1) hydrophobicity, 2) α -helical, or 3) β -strand periodicity, or the density of 4) positive charge, 5) negative charge, 6) serine, 7) threonine, 8) proline, 9) glycine, 10) amphiphilic, or 11) aromatic residues.
Signal peptide features	5	SP scores	Each score is computed in the putative signal peptide region defined by a sliding widow method search within 90 N-terminal residues for: the density of 1) positive charge, 2,3) two kinds of the density of negative charge, or the mean of 4) hydrophobicity, and 5) cleavage site preference residues.

Amphiphilic alpha helix	1	PA score: $\frac{\mu_H - \mu_C r \cos A}{n}$	For 30 N-terminal residues of the input sequence, the segments between 10 and 20 residues are generated by the sliding window method. For each segment, the score is computed from μ_H (magnitude of a hydrophobic moment vector) and μ_C (magnitude of a charge moment vector) by a formula as shown in the left column, and the best segment score is picked up as the PA score. n is the size of the window, r is the ratio parameter between μ_H and μ_C , and A is the angle between the two vectors.
Hexamer motifs	15	Motif scores: $-\log_{10}(p)$ Total score	Motifs are the 14 hexamer motifs that are significantly and frequently observed in the mitochondrial proteins compared to the non-mitochondrial ones ($p < 10^{-5}$.) The total score is the sum of each motif score.
Cleavage site features	2	Cleavage scores	For 100 N-terminal residues of the input sequence, 10 residue segments are generated by the sliding window method. For each segment, the cleavage score is calculated as the sum of position weighted matrix (PWM) scores for 10 residues, and the best and the second-best cleavage scores are picked up. The PWM is a given matrix in the Mitofates program.

526 3.2.4. Training and prediction method

527 I adopted GBM, one of the ensemble learning algorithms, and created predictors using
 528 xgboost (Chen & Guestrin, 2016) package in R (R Core Team, 2018) for the Mit and
 529 MRO datasets (Mit Predictor and MRO predictor). GBM reconstructs the unknown
 530 functional dependence $x \xrightarrow{f} y$ with estimate $\hat{f}(x)$; x is the explanatory input
 531 variables, y is the corresponding label. The scheme of the algorithm is shown in Figure
 532 3-3 (based on Natekin & Knoll, 2013). Xgboost chooses decision tree as the base-
 533 learner.

		Friedman's Gradient Boost Algorithm (based on Natekin & Knoll, 2013)
$(x, y)_{i=1}^N$	Input data	
x	Input variable	
y	Corresponding label	1. initialize \hat{f}_0 with a constant
N	Dataset size	2. for $t = 1$ to M do
M	Number of iterations	3. compute the negative gradient $g_t(x)$
$\Psi(y, f)$	Loss function	4. fit a new base-learner function $h(x, \theta_t)$
$g(x)$	Negative gradient	5. find the best gradient descent step-size ρ_t :
$h(x, \theta)$	Base-learner model (xgboost: Decision tree)	$\rho_t = \arg \min_{\rho} \sum_{i=1}^N \Psi [y_i, \hat{f}_{t-1}(x_i) + \rho h(x_i, \theta_t)]$
θ	Parameter	6. update the function estimate:
ρ	Step-size	$\hat{f}_t \leftarrow \hat{f}_{t-1} + \rho_t h(x, \theta_t)$
534		7. end for

535 Figure 3-3: The scheme of the algorithm of GBM.

536 I searched for optimal values of logical variables employed in the xgboost
 537 algorithm. Parameters for tree boosting, learning rate (*eta*), maximum depth of a tree
 538 (*max_depth*), minimum sum of instance weight (*min_child_weight*), maximum delta
 539 step (*max_delta_step*), and gamma were tuned with grid search, and finally I determined
 540 to set the default values for these variables. In addition, I optimized the parameter of the

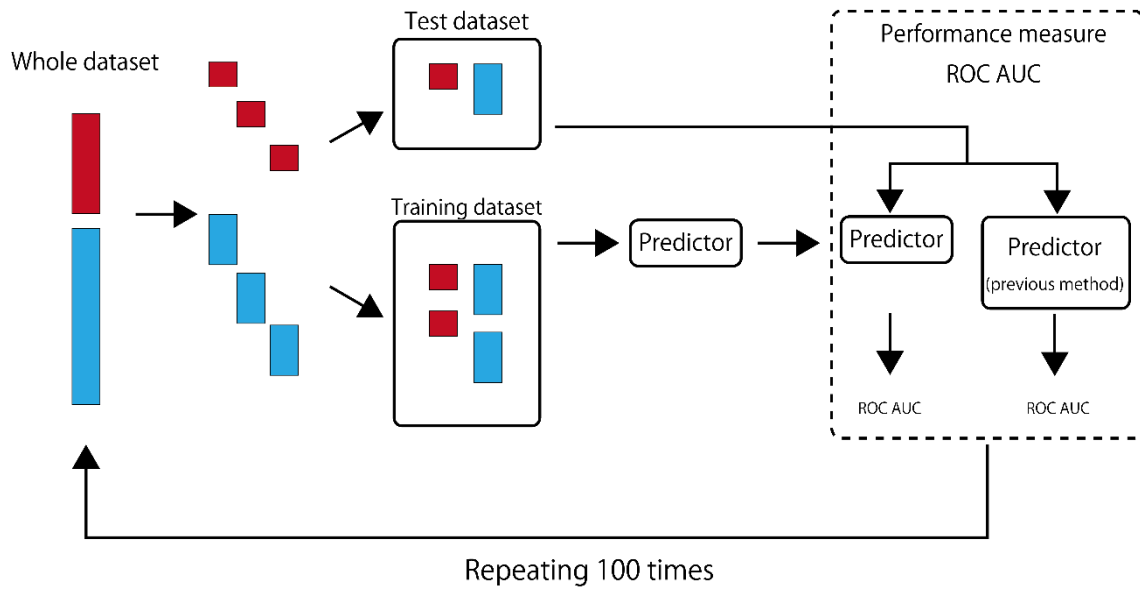
541 number of trees to the model by cross-validation. For other parameters, I used the
542 default value.

543 3.2.5. Performance measures

544 To evaluate the performances of both the NommPred predictors—Mit Predictor and
545 MRO Predictor—a receiver operating characteristics (ROC) curve and a ROC area
546 under the curve (AUC) (Bradley, 1997) were used. In the R system, the ROC curve was
547 drawn by plotting the true positive rate (y-axis) against the false positive rate (x-axis)
548 for different cut-off values, and the ROC AUC was drawn based on the ROC curve.

549 To evaluate the robustness of the ROC AUC measures, I randomly divided the
550 Mit or MRO dataset into three subsets (three-fold cross-validation), and I used two of
551 them for the training data, and the other for the test data. This process was repeated 100
552 times (Figure 3-4).

553 To compare NommPred with a previous predictor, Mitofates, I used the same
554 test data as that of NommPred for Mitofates to evaluate its performance. In this
555 performance comparison, I carried out the paired t test and Wilcoxon signed rank test to
556 evaluate the difference between the means of these 100 paired ROC AUC scores.



557

558

Figure 3-4: The scheme of the three-fold cross validation.

559

560 3.3. Results

561 3.3.1. Performance comparison analysis

562 **Prediction of mitochondrial proteins**

563 I carried out the performance comparison analysis between NommPred and a previous
564 method, Mitofates. A dataset including the mitochondrial and non-mitochondrial
565 proteins of seven non-model organismal taxonomic groups was used for the preparation
566 of the training and test datasets (as described in the Materials and Methods section),
567 resulting in the creation of Mit Predictor. Performance measure scores are listed in Table
568 3-3 and shown by boxplot in Figure 3-5.

Table 3-3: Comparison of the mean ROC AUC scores between NommPred and Mitofates. In NommPred mitochondrial proteins were predicted by Mit Predictor, while MRO proteins were by MRO Predictor. 100 randomly generated datasets ($n = 100$) of mitochondrial or MRO proteins were used for cross-validation (see Materials and Methods).

569

Prediction target	ROC AUC		<i>p value</i>	
	NommPred	Mitofates	Paired <i>t</i> test	Wilcoxon signed rank test
Mitochondrial protein	0.9463	0.9080	1.62E-42	0.00E+00
MRO protein	0.9041	0.8021	6.86E-40	0.00E+00

570

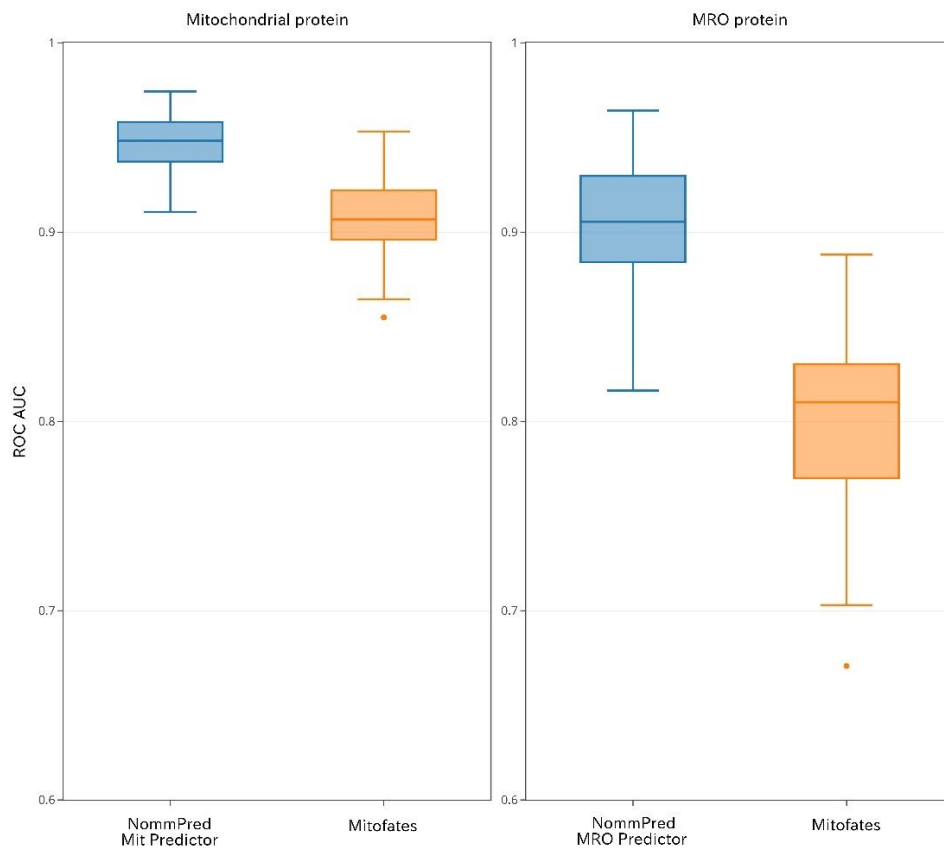
571

572

573

574

575



576

577

Figure 3-5: Boxplots showing the performance of the predictors of the mitochondrial and MRO proteins. The ROC AUC scores of 100 randomly generated datasets (y-axis) of the two predictors are plotted for, NommPred (Mit Predictor or/and MRO Predictor) in NommPred, and Mitofates (x-axis), are plotted. Lines within the boxplot indicate the median, the lower/higher quartile (Q1/Q3), and lower/higher whiskers.

578

579 For the mean ROC AUC scores (sample size $n = 100$), Mitofates achieved 0.9080,
580 whereas the performance of Mit Predictor of NommPred was superior with a value of
581 0.9463 (Table 3-3). Moreover, the difference between the two mean ROC AUC scores
582 was significant (paired t test: p value = 1.618×10^{-42} , Wilcoxon signed rank test: p value
583 = ~ 0).

584 Generally, the ROC AUC score ranging between 0.5 and 0.7 is regarded as less
585 accurate, between 0.7 and 0.9 as moderately accurate, and more than 0.9 as highly
586 accurate (Fischer et al., 2003). Based on these criteria, Mitofates still showed sufficient
587 accuracy in the prediction of the mitochondrial proteins derived from non-model
588 organisms. However, for the prediction of those proteins, Mit Predictor with a higher
589 ROC AUC score was preferred.

590 **Prediction of MRO proteins**

591 As described in the Materials and Methods section, I classified the entire dataset into
592 two—Mit and MRO (Table 3-1). The MRO dataset including the MRO and non-MRO
593 proteins of three non-model organismal groups was used for the preparation of the
594 training and test datasets (described in the Materials and Methods section), resulting in
595 the creation of MRO Predictor. I carried out a similar comparison analysis between the
596 performance of MRO Predictor and that of Mitofates for the prediction of the MRO
597 proteins. The performance measure scores are listed in Table 3-3.

598 Mitofates achieved a mean ROC AUC score (sample size $n = 100$) of 0.8021,
599 whereas the performance of the MRO predictor of NommPred was far better with a
600 mean value of 0.9041 (paired t test: p value = 6.855×10^{-40} , Wilcoxon signed rank test:
601 p value = ~ 0) (Table 3-3). Based on these results, MRO Predictor of NommPred is
602 suitable for the MRO proteins.

603 3.4. Discussions

604 I succeeded in developing NommPred, the predictors for the mitochondrial and MRO
605 proteins derived from diverse non-model organisms, except for those belonging to
606 Metazoa, Embryophyta and Fungi. Previously, the protein sequence data derived from
607 non-model organisms were subjected to the predictor trained only by using the data
608 from model organisms. NommPred could resolve the problem resulted from such
609 inconsistency between the origins of the training data (model organisms) and the input
610 data (non-model organisms).

611 3.4.1. Performance comparison analysis

612 The results of the statistical analysis (Table 3-3) clearly supported the superiority of
613 NommPred in the performance of predicting the mitochondrial proteins of non-model
614 organisms when compared to the existing best method, Mitofates. In particular,
615 NommPred is the first software that is expected to be used for predicting the MRO
616 proteins. NommPred would be useful for the prediction of metabolic pathways relating
617 to the mitochondria/MROs from non-model organisms, the NGS data of which can be
618 available. Since there is no other predictor suitable for the prediction of MRO proteins,
619 MRO predictor in NommPred is useful tool to search for putative MRO proteins.

620 In this study, I retrieved almost all protein sequence data whose cellular
621 localization were experimentally verified to mitochondria/MROs from various sequence
622 databases. However, the origins of the sequence data of mitochondrial/MRO proteins in
623 the entire dataset (Table 3-1) are biased for those of the parasitic organisms. Therefore,
624 taxon sampling of our dataset is still very sparse. The accumulation of more data of the
625 mitochondrial/MRO proteins of non-model organisms, especially from the free-living
626 ones whose localization was confirmed experimentally, is essential to further improve

627 the predictors presented in this work. I should continuously make efforts toward
628 updating the dataset to provide more accurate predictors. Although NommPred may still
629 have some problems that need to be improved in the future, I hope it will be helpful for
630 the prediction of the mitochondrial/MRO proteins of non-model organisms.
631

964 Acknowledgements

965 I would like to express the deepest appreciation to my supervisor, Professor Tetsuo
966 Hashimoto (University of Tsukuba) and Professor Yuji Inagaki (University of Tsukuba)
967 for their support and encouragement during my PhD program period. I am deeply
968 grateful to Professor Toshiyuki Amagasa (University of Tsukuba) and Professor
969 Hiroyuki Kitagawa (University of Tsukuba) for accepting me as a student of master's
970 program in computer science using Graduate School Dual Degree Program of university
971 of Tsukuba, and contributing to develop my prediction software. Assistant Professor
972 Ryoma Kamikawa (Kyoto University) for training in the earlier stage on my career.
973 Doctor Goro Tanifuji (National Museum of Nature and Science), Assistant Professor
974 Takuro Nakayama (Tohoku University) and Doctor Yoshiyuki Ishitani gave me a lot of
975 insight comments and suggestions.
976 Finally, I want to thank all the member of Molecular Evolution of Microbes (Hashimoto
977 & Inagaki laboratory at University of Tsukuba) and Kitagawa Data Engineering
978 (University of Tsukuba) for their help.

979 References

- 980 1. Adl SM, Bass D, Lane CE, et al. Revisions to the Classification, Nomenclature, and
981 Diversity of Eukaryotes. *J Eukaryot Microbiol.* 2018. doi:10.1111/jeu.12691.
- 982 2. Altschul SF, Gish W, Miller W, Myers EW, Lipman DJ. A basic local alignment
983 search tool. *J Mol Biol.* 1990;215:403–410. doi:10.1016/S0022-2836(05)80360-2.
- 984 3. Andersson SG, Zomorodipour A, Andersson JO, et al. The genome sequence of
985 *Rickettsia prowazekii* and the origin of mitochondria. *Nature.* 1998;396(6707):133-
986 40. doi:10.1038/24094.
- 987 4. Arthur D & Vassilvitskii S. k-means++: The advantages of careful seeding.
988 Proceedings of the Eighteenth Annual ACM - SIAM Symposium on Discrete
989 Algorithms. 2007;1027-35.
- 990 5. Aurrecochea C, Brestelli J, Brunk BP, et al. GiardiaDB and TrichDB: integrated
991 genomic resources for the eukaryotic protist pathogens *Giardia lamblia* and
992 *Trichomonas vaginalis*. *Nucleic Acids Res.* 2009;37(Database issue):D526-30.
993 doi:10.1093/nar/gkn631.
- 994 6. Barnett DW, Garrison EK, Quinlan AR, Strömberg MP, Marth GT. BamTools: a
995 C++ API and toolkit for analyzing and managing BAM files. *Bioinformatics.*
996 2011;27(12):1691-2. doi:10.1093/bioinformatics/btr174.
- 997 7. Beltrán NC, Horváthová L, Jedelský PL, et al. Iron-induced changes in the
998 proteome of *Trichomonas vaginalis* hydrogenosomes. *PLoS One.*
999 2013;8(5):e65148. doi:10.1371/journal.pone.0065148.
- 1000 8. Benson DA, Cavanaugh M, Clark K, et al. GenBank. *Nucleic Acids Res.*
1001 2018;46(D1):D41-D47. doi:10.1093/nar/gkx1094.

- 1002 9. Bradley AP. The use of the area under the ROC curve in the evaluation of machine
1003 learning algorithms. *Pattern Recognit.* 1997;30(7):1145-59. doi:10.1016/S0031-
1004 3203(96)00142-2.
- 1005 10. Brindefalk B, Ettema TJ, Viklund J, Thollesson M, Andersson SG. A
1006 phylometagenomic exploration of oceanic alphaproteobacteria reveals
1007 mitochondrial relatives unrelated to the SAR11 clade. *PLoS One.*
1008 2011;6(9):e24457. doi:10.1371/journal.pone.0024457.
- 1009 11. Camacho C, Coulouris G, Avagyan V, et al. Blast+: architecture and applications.
1010 *BMC bioinformatics.* 2009;10(1):421. doi:10.1186/1471-2105-10-421.
- 1011 12. Capella-Gutiérrez S, Silla-Martínez JM, Gabaldón T. trimAl: a tool for automated
1012 alignment trimming in large-scale phylogenetic analyses. *Bioinformatics.*
1013 2009;25(15):1972-3. doi:10.1093/bioinformatics/btp348.
- 1014 13. Carlton JM, Hirt RP, Silva JC, et al. Draft genome sequence of the sexually
1015 transmitted pathogen *Trichomonas vaginalis*. *Science.* 2007;315(5809):207-12.
1016 doi:10.1126/science.1132894.
- 1017 14. Chen T, Guestrin C. A scalable tree boosting system. eprint arXiv. 2016.
1018 doi:10.1145/2939672.2939785.
- 1019 15. Chen X, Li J, Hou J, Xie Z, Yang F. Mammalian mitochondrial proteomics: insights
1020 into mitochondrial functions and mitochondria-related diseases. *Expert Rev*
1021 *Proteomics.* 2010;7(3):333-45. doi:10.1586/epr.10.22.
- 1022 16. Cherry JM, Hong EL, Amundsen C, et al. *Saccharomyces* genome database: the
1023 genomics resource of budding yeast. *Nucleic Acids Res.* 2012;40(D1):D700-5.
1024 doi:10.1093/nar/gkr1029.

- 1025 17. Cortes C & Vapnik V. Support-vector networks. *Mach Learn.* 1995;20(3):273-97.
1026 doi:10.1007/BF00994018.
- 1027 18. Eddy SR. A New Generation of Homology Search Tools Based on Probabilistic
1028 Inference. *Genome Inform.* 2009;23(1):205-11. doi:10.1142/9781848165632_0019.
- 1029 19. Emanuelsson O, Brunak S, von Heijne G, Nielsen H. Locating proteins in the cell
1030 using TargetP, SignalP and related tools. *Nat Protoc.* 2007;2(4):953-71.
1031 doi:10.1038/nprot.2007.131.
- 1032 20. Embley TM & Martin W. Eukaryotic evolution, changes and challenges. *Nature.*
1033 2006;440(7084):623-30. doi:10.1038/nature04546.
- 1034 21. Fang YK, Chien KY, Huang KY, et al. Responding to a Zoonotic Emergency with
1035 Multi-omics Research: *Pentatrichomonas hominis* Hydrogenosomal Protein
1036 Characterization with Use of RNA Sequencing and Proteomics. *OMICS.*
1037 2016;20(11):662-669. doi:10.1089/omi.2016.0111.
- 1038 22. Finn RD, Bateman A, Clements J, et al. Pfam: the protein families database.
1039 *Nucleic Acids Res.* 2014;42(Database issue):D222-30. doi:10.1093/nar/gkt1223.
- 1040 23. Fischer JE, Bachmann LM, Jaeschke R. A readers' guide to the interpretation of
1041 diagnostic test properties: clinical example of sepsis. *Intensive Care Med.*
1042 2003;29(7):1043-51. doi:10.1007/s00134-003-1761-8.
- 1043 24. Friedman J, Hastie T, Tibshirani R. Additive logistic regression: a statistical view of
1044 boosting. *Ann Statist.* 2000;28(2):337-407. doi:10.1214/aos/1016218223.
- 1045 25. Friedman JH. Greedy function approximation: a gradient boosting machine. *Ann*
1046 *Statist.* 1999;29(5):1189-232. doi:10.1214/aos/1013203451.
- 1047 26. Friedman JH. Stochastic gradient boosting. *Comput Stat Data An.* 2002;38(4):367-
1048 78. doi:10.1016/S0167-9473(01)00065-2.

- 1049 27. Fu L, Niu B, Zhu Z, Wu S, Li W. CD-HIT: accelerated for clustering the next-
1050 generation sequencing data. *Bioinformatics*. 2012. 28(23):3150-2.
1051 doi:10.1093/bioinformatics/bts565.
- 1052 28. Fukasawa Y, Tsuji J, Fu SC, Tomii K, Horton P, Imai K. MitoFates: improved
1053 prediction of mitochondrial targeting sequences and their cleavage sites. *Mol Cell*
1054 *Proteomics*. 2015;14(4):1113-26. doi:10.1074/mcp.M114.043083.
- 1055 29. Gonczarowska-Jorge H, Zahedi RP, Sickmann A. The proteome of baker's yeast
1056 mitochondria. *Mitochondrion*. 2017;33:15-21. doi:10.1016/j.mito.2016.08.007.
- 1057 30. Grabherr MG, Haas BJ, Yassour M, et al. Full-length transcriptome assembly from
1058 RNA-Seq data without a reference genome. *Nat Biotechnol*. 2011;29(7):644-52.
1059 doi:10.1038/nbt.1883.
- 1060 31. Gray MW. Mitochondrial Evolution. *Cold Spring Harb Perspect Biol*. 2012;4(9):
1061 a011403. doi:10.1101/cshperspect.a011403.
- 1062 32. Haas BJ, Papanicolaou A, Yassour M, et al. De novo transcript sequence
1063 reconstruction from RNA-seq using the Trinity platform for reference generation
1064 and analysis. *Nat Protoc*. 2013;8(8):1494-512. doi:10.1038/nprot.2013.084.
- 1065 33. Hagen KD, Hirakawa MP, House SA, et al. Novel structural components of the
1066 ventral disc and lateral crest in *Giardia intestinalis*. *PLoS Negl Trop Dis*.
1067 2011;5(12):e1442. doi:10.1371/journal.pntd.0001442.
- 1068 34. Hoang DT, Chernomor O, von Haeseler A, Minh BQ, Vinh LS. UFBoot2:
1069 Improving the Ultrafast Bootstrap Approximation. *Mol Biol Evol*. 2018;35(2):518-
1070 522. doi:10.1093/molbev/msx281.
- 1071 35. Hoff KJ, Lange S, Lomsadze A, Borodovsky M, Stanke M. BRAKER1:
1072 unsupervised RNA-Seq-based genome annotation with GeneMark-ET and

- 1073 AUGUSTUS. *Bioinformatics*. 2015;32(5):767-769.
1074 doi:10.1093/bioinformatics/btv661.
- 1075 36. Hrdy I, Hirt RP, Dolezal P, et al. *Trichomonas* hydrogenosomes contain the NADH
1076 dehydrogenase module of mitochondrial complex I. *Nature*. 2004;432(7017):618-
1077 22. doi:10.1038/nature03149.
- 1078 37. Jedelský PL, Doležal P, Rada P, et al. The minimal proteome in the reduced
1079 mitochondrion of the parasitic protist *Giardia intestinalis*. *PLoS One*.
1080 2011;6(2):e17285. doi:10.1371/journal.pone.0017285.
- 1081 38. Jerlström-Hultqvist J, Einarsson E, Xu F, et al. Hydrogenosomes in the diplomonad
1082 *Spironucleus salmonicida*. *Nat Commun*. 2013;1.897916667.
1083 doi:10.1038/ncomms3493.
- 1084 39. Jerlström-Hultqvist J, Franzén O, Ankarklev J, et al. Genome analysis and
1085 comparative genomics of a *Giardia intestinalis* assemblage E isolate. *BMC*
1086 *Genomics*. 2010;0.835416667. doi:10.1186/1471-2164-11-543.
- 1087 40. Jones P, Binns D, Chang HY, et al. InterProScan 5: genome-scale protein function
1088 classification. *Bioinformatics*. 2014;30(9):1236-40.
1089 doi:10.1093/bioinformatics/btu031.
- 1090 41. Kalyaanamoorthy S, Minh BQ, Wong TKF, von Haeseler A, Jermini LS.
1091 ModelFinder: fast model selection for accurate phylogenetic estimates. *Nat*
1092 *Methods*. 2017;14(6):587-589. doi:10.1038/nmeth.4285.
- 1093 42. Kanehisa M, Sato Y, Morishima K. BlastKOALA and GhostKOALA: KEGG Tools
1094 for Functional Characterization of Genome and Metagenome Sequences. *J Mol*
1095 *Biol*. 2016;428(4):726-731. doi:10.1016/j.jmb.2015.11.006.

- 1096 43. Karnkowska A, Vacek V, Zubáčová Z, et al. A Eukaryote without a Mitochondrial
1097 Organelle. *Curr Biol.* 2016;26(10):1274-84. doi:10.1016/j.cub.2016.03.053.
- 1098 44. Katoh K & Standley DM. MAFFT multiple sequence alignment software version 7:
1099 improvements in performance and usability. *Mol Biol Evol.* 2013;30(4):772-80.
1100 doi:10.1093/molbev/mst010.
- 1101 45. Kim D, Pertea G, Trapnell C, Pimentel H, Kelley R, Salzberg SL. TopHat2:
1102 accurate alignment of transcriptomes in the presence of insertions, deletions and
1103 gene fusions. *Genome Biol.* 2013;14(4): R36. doi:10.1186/gb-2013-14-4-r36.
- 1104 46. Kolisko M, Silberman JD, Cepicka I, et al. A wide diversity of previously
1105 undetected free-living relatives of diplomonads isolated from marine/saline
1106 habitats. *Environ Microbiol.* 2010;12(10):2700-10. doi:10.1111/j.1462-
1107 2920.2010.02239.x.
- 1108 47. Kumar A, Agarwal S, Heyman JA, et al. Subcellular localization of the yeast
1109 proteome. *Genes Dev.* 2002;16(6):707-19. doi:10.1101/gad.970902.
- 1110 48. Kumar S, Jones M, Koutsovoulos G, Clarke M, Blaxter M. Blobology: exploring
1111 raw genome data for contaminants, symbionts and parasites using taxon-annotated
1112 GC-coverage plots. *Front Genet.* 2013;0.33125. doi:10.3389/fgene.2013.00237.
- 1113 49. Leger MM, Kolisko M, Kamikawa R, et al. Organelles that illuminate the origins of
1114 *Trichomonas* hydrogenosomes and *Giardia* mitosomes. *Nat Ecol Evol.*
1115 2017;1(4):0092. doi:10.1038/s41559-017-0092.
- 1116 50. Leinonen R, Sugawara H, Shumway M. The Sequence Read Archive. *Nucleic*
1117 *Acids Res.* 2011;39(Database issue):D19-21. doi:10.1093/nar/gkq1019.

- 1118 51. Li H, Handsaker B, Wysoker A, et al. The Sequence Alignment/Map format and
1119 SAMtools. *Bioinformatics*. 2009;25(16):2078-9.
1120 doi:10.1093/bioinformatics/btp352.
- 1121 52. Lindmark DG & Müller M. Hydrogenosome, a cytoplasmic organelle of the
1122 anaerobic flagellate *Tritrichomonas foetus*, and its role in pyruvate metabolism. *J*
1123 *Biol Chem*. 1973;248(22):7724-8.
- 1124 53. Lomsadze A, Burns PD, Borodovsky M. Integration of mapped RNA-Seq reads
1125 into automatic training of eukaryotic gene finding algorithm. *Nucleic Acids Res*.
1126 2014;42(15):e119. doi:10.1093/nar/gku557.
- 1127 54. Lomsadze A, Ter-Hovhannisyan V, Chernoff YO, Borodovsky M. Gene
1128 identification in novel eukaryotic genomes by self-training algorithm. *Nucleic*
1129 *Acids Res*. 2005;33(20): 6494–6506. doi:10.1093/nar/gki937.
- 1130 55. Makiuchi T, Nozaki T. Highly divergent mitochondrion-related organelles in
1131 anaerobic parasitic protozoa. *Biochimie*. 2014;100:3-17.
1132 doi:10.1016/j.biochi.2013.11.018.
- 1133 56. Martijn J, Vosseberg J, Guy L, Offre P, Ettema TJG. Deep mitochondrial origin
1134 outside the sampled alphaproteobacteria. *Nature*. 2018;557(7703):101-105.
1135 doi:10.1038/s41586-018-0059-5.
- 1136 57. Martin WF, Roettger M, Ku C, Garg SG, Nelson-Sathi S, Landan G. Late
1137 Mitochondrial Origin Is an Artifact. *Genome Biol Evol*. 2017;9(2):373-379.
1138 doi:10.1093/gbe/evx027.
- 1139 58. Millet CO, Williams CF, Hayes AJ, Hann AC, Cable J, Lloyd D. Mitochondria-
1140 derived organelles in the diplomonad fish parasite *Spironucleus vortens*. *Exp*
1141 *Parasitol*. 2013;135(2):262-73. doi:10.1016/j.exppara.2013.07.003.

- 1142 59. Morrison HG, McArthur AG, Gillin FD, et al. Genomic minimalism in the early
1143 diverging intestinal parasite *Giardia lamblia*. *Science*. 2007;317(5846):1921-6.
1144 doi:10.1126/science.1143837.
- 1145 60. Müller M, Mentel M, van Hellemond JJ, et al. Biochemistry and evolution of
1146 anaerobic energy metabolism in eukaryotes. *Microbiol Mol Biol Rev*.
1147 2012;76(2):444-95. doi:10.1128/MMBR.05024-11.
- 1148 61. Natekin A & Knoll A. Gradient boosting machines, a tutorial. *Front Neurobot*.
1149 2013;7:21. doi:10.3389/fnbot.2013.00021.
- 1150 62. Nguyen LT, Schmidt HA, von Haeseler A, Minh BQ. IQ-TREE: a fast and effective
1151 stochastic algorithm for estimating maximum-likelihood phylogenies. *Mol Biol*
1152 *Evol*. 2015;32(1):268-74. doi:10.1093/molbev/msu300.
- 1153 63. Nurk S, Meleshko D, Korobeynikov A, Pevzner PA. metaSPAdes: a new versatile
1154 metagenomic assembler. *Genome Res*. 2017;27(5):824-834.
1155 doi:10.1101/gr.213959.116.
- 1156 64. Park JS, Kolisko M, Heiss AA, Simpson AG. Light microscopic observations,
1157 ultrastructure, and molecular phylogeny of *Hicanonectes teleskopos* n. g., n. sp., a
1158 deep-branching relative of diplomonads. *J Eukaryot Microbiol*. 2009;56(4):373-84.
1159 doi:10.1111/j.1550-7408.2009.00412.x.
- 1160 65. Peña-Díaz P & Lukeš J. Fe–S cluster assembly in the supergroup Excavata. *J Biol*
1161 *Inorg Chem*. 2018;23(4):521-541. doi:10.1007/s00775-018-1556-6.
- 1162 66. Pittis AA & Gabaldón T. Late acquisition of mitochondria by a host with chimaeric
1163 prokaryotic ancestry. *Nature*. 2016;531:101–104. doi:10.1038/nature16941.
- 1164 67. R Core Team. R: A language and environment for statistical computing.
1165 2018;https://www.R-project.org/.

- 1166 68. Rada P, Doležal P, Jedelský PL, et al. The core components of organelle biogenesis
1167 and membrane transport in the hydrogenosomes of *Trichomonas vaginalis*. PLoS
1168 One. 2011;6(9):e24428. doi:10.1371/journal.pone.0024428.
- 1169 69. Reinders J, Zahedi RP, Pfanner N, Meisinger C, Sickmann A. Toward the complete
1170 yeast mitochondrial proteome: multidimensional separation techniques for
1171 mitochondrial proteomics. J Proteome Res. 2006;5(7):1543-54.
1172 doi:10.1021/pr050477f.
- 1173 70. Roger AJ, Muñoz-Gómez SA, Kamikawa R. The Origin and Diversification of
1174 Mitochondria. Curr Biol. 2017;27(21):R1177-R1192.
1175 doi:10.1016/j.cub.2017.09.015.
- 1176 71. Savojardo C, Martelli PL, Fariselli P, Casadio R. TPpred2: improving the prediction
1177 of mitochondrial targeting peptide cleavage sites by exploiting sequence motifs.
1178 Bioinformatics. 2014;30(20):2973-4. doi:10.1093/bioinformatics/btu411.
- 1179 72. Savojardo C, Martelli PL, Fariselli P, Casadio R. TPpred3 detects and discriminates
1180 mitochondrial and chloroplastic targeting peptides in eukaryotic proteins.
1181 Bioinformatics. 2015;31(20):3269-75. doi:10.1093/bioinformatics/btv367.
- 1182 73. Schneider RE, Brown MT, Shiflett AM, et al. The *Trichomonas vaginalis*
1183 hydrogenosome proteome is highly reduced relative to mitochondria, yet complex
1184 compared with mitosomes. Int J Parasitol. 2011;41(13-14):1421-34.
1185 doi:10.1016/j.ijpara.2011.10.001.
- 1186 74. Chen S, Zhou Y, Chen Y, Gu J. fastp: an ultra-fast all-in-one FASTQ preprocessor.
1187 Bioinformatics. 2017;Volume 34, Issue 17, Pages i884–i890.
1188 doi:10.1093/bioinformatics/bty560.

- 1189 75. Sickmann A, Reinders J, Wagner Y, et al. The proteome of *Saccharomyces*
1190 *cerevisiae* mitochondria. Proc Natl Acad Sci U S A. 2003;100(23):13207-12.
1191 doi:10.1073/pnas.2135385100.
- 1192 76. Simpson AG. Cytoskeletal organization, phylogenetic affinities and systematics in
1193 the contentious taxon Excavata (Eukaryota). Int J Syst Evol Microbiol. 2003;53(Pt
1194 6):1759-77. doi:10.1099/ijs.0.02578-0.
- 1195 77. SRA Toolkit Development Team. <http://ncbi.github.io/sra-tools/>.
- 1196 78. Stanke M, Diekhans M, Baertsch R, Haussler D. Using native and syntenically
1197 mapped cDNA alignments to improve de novo gene finding. Bioinformatics. 2008.
1198 doi:10.1093/bioinformatics/btn013.
- 1199 79. Stanke M, Schöffmann O, Morgenstern B, Waack S. Gene prediction in eukaryotes
1200 with a generalized hidden Markov model that uses hints from external sources.
1201 BMC Bioinformatics. 2006;0.334722222. doi:10.1186/1471-2105-7-62.
- 1202 80. Suzuki S, Kakuta M, Ishida T, Akiyama Y. GHOSTX: an improved sequence
1203 homology search algorithm using a query suffix array and a database suffix array.
1204 PLoS One. 2014;9(8):e103833. doi:10.1371/journal.pone.0103833.
- 1205 81. Takishita K, Kolisko M, Komatsuzaki H, et al. Multigene phylogenies of diverse
1206 Carpediemonas-like organisms identify the closest relatives of 'amitochondriate'
1207 diplomonads and retortamonads. Protist. 2012;163(3):344-55.
1208 doi:10.1016/j.protis.2011.12.007.
- 1209 82. Tanifuji G, Takabayashi S, Kume K, et al. The draft genome of *Kipferlia bialata*
1210 reveals reductive genome evolution in fornicate parasites. PLoS One.
1211 2018;13(3):e0194487. doi:10.1371/journal.pone.0194487.

- 1212 83. Ter-Hovhannisyan V, Lomsadze A, Chernoff YO, Borodovsky M. Gene prediction
1213 in novel fungal genomes using an ab initio algorithm with unsupervised training.
1214 Genome Res. 2008;18(12):1979-90. doi:10.1101/gr.081612.108.
- 1215 84. Thomas PD, Campbell MJ, Kejariwal A, et al. PANTHER: a library of protein
1216 families and subfamilies indexed by function. Genome Res. 2003;13(9):2129-41.
1217 doi:10.1101/gr.772403.
- 1218 85. Tovar J, León-Avila G, Sánchez LB, et al. Mitochondrial remnant organelles of
1219 *Giardia* function in iron-sulphur protein maturation. Nature. 2003;426(6963):172-6.
1220 doi:10.1038/nature01945.
- 1221 86. Trapnell C, Pachter L, Salzberg SL. TopHat: discovering splice junctions with
1222 RNA-Seq. Bioinformatics. 2009;25(9): 1105–1111.
1223 doi:10.1093/bioinformatics/btp120.
- 1224 87. UniProt C. UniProt: the universal protein knowledgebase. Nucleic Acids Res.
1225 2017;45(D1):D158-69. doi:10.1093/nar/gkw1099.
- 1226 88. Vacek V, Novák LVF, Treitli SC, et al. Fe-S Cluster Assembly in Oxymonads and
1227 Related Protists. Mol Biol Evol. 2018;35(11):2712-2718.
1228 doi:10.1093/molbev/msy168.
- 1229 89. van Grinsven KW, Rosnowsky S, van Weelden SW, et al. Acetate:succinate CoA-
1230 transferase in the hydrogenosomes of *Trichomonas vaginalis*: identification and
1231 characterization. J Biol Chem. 2008. 283(3):1411-8. doi:10.1074/jbc.M702528200.
- 1232 90. Waterhouse RM, Seppey M, Simão FA, et al. BUSCO applications from quality
1233 assessments to gene prediction and phylogenomics. Mol Biol Evol.
1234 2017;35(3):543–548. doi:10.1093/molbev/msx319.

- 1235 91. Williams KP, Sobral BW, Dickerman AW. A robust species tree for the
1236 alphaproteobacteria. *J Bacteriol.* 2007;189(13):4578-86. doi:10.1128/JB.00269-07.
- 1237 92. Wilson D, Pethica R, Zhou Y, et al. SUPERFAMILY - Comparative Genomics,
1238 Datamining and Sophisticated Visualisation. *Nucleic Acids Res.* 2009;37(Database
1239 issue):D380-6. doi:10.1093/nar/gkn762.
- 1240 93. Wood DE, Salzberg SL. Kraken: ultrafast metagenomic sequence classification
1241 using exact alignments. *Genome Biol.* 2014;15(3):R46. doi:10.1186/gb-2014-15-3-
1242 r46.
- 1243 94. Woodcroft BJ, Scanlon KL, Doyle M, Speed T, Ralph SA. ApiLoc - A database of
1244 published protein sub-cellular localisation in Apicomplexa (version 3). 2011.
1245 <http://apiloc.biochem.unimelb.edu.au/apiloc/apiloc>. Updated 2011. Accessed June
1246 11, 2016.
- 1247 95. Yubuki N, Inagaki Y, Nakayama T, Inouye I. Ultrastructure and ribosomal RNA
1248 phylogeny of the free-living heterotrophic flagellate *Dysnectes brevis* n. gen., n. sp.,
1249 a new member of the Fornicata. *J Eukaryot Microbiol.* 2007;54(2):191-200.
1250 doi:10.1111/j.1550-7408.2007.00252.x.
- 1251 96. Yubuki N, Simpson AG, Leander BS. Comprehensive ultrastructure of *Kipferlia*
1252 *bialata* provides evidence for character evolution within the Fornicata (Excavata).
1253 *Protist.* 2013;164(3):423-39. doi:10.1016/j.protis.2013.02.002.
- 1254 97. Zhang Q, Táborský P, Silberman JD, Pánek T, Čepička I, Simpson AG. Marine
1255 Isolates of *Trimastix marina* Form a Plesiomorphic Deep-branching Lineage within
1256 Preaxostyla, Separate from Other Known Trimastigids (*Paratrimastix* n. gen.).
1257 *Protist.* 2015;166(4):468-91. doi:10.1016/j.protis.2015.07.003.

1258 98. Zubáčová Z, Novák L, Bublíková J, et al. The mitochondrion-like organelle of
1259 *Trimastix pyriformis* contains the complete glycine cleavage system. PLoS One.
1260 2013;8(3):e55417. doi:10.1371/journal.pone.0055417.